

# Application of nanodiamond-polymer composite holographic gratings in a very cold neutron interferometer

Sonja Falmbigl,<sup>1</sup> Roxana H. Ackermann,<sup>1</sup> Elhoucine Hadden,<sup>2,\*</sup> Hanno Filter-Pieler,<sup>1</sup> Tobias Jenke,<sup>1</sup> Jürgen Klepp,<sup>1</sup> Christian Pruner,<sup>3</sup> Yasuo Tomita,<sup>4</sup> and Martin Fally<sup>1,†</sup>

<sup>1</sup>*Faculty of Physics, University of Vienna, Wien, Austria*

<sup>2</sup>*Institut Laue-Langevin, Grenoble, France*

<sup>3</sup>*Faculty of Natural and Life Sciences, Department of Chemistry and Physics of Materials, University of Salzburg, Austria*

<sup>4</sup>*Department of Engineering Science, University of Electro-Communications, Tokyo, Japan*

In recent decades, photosensitive materials have been used for the development of optical devices not only for light, but also for cold and very cold neutrons. We show that holographically recorded gratings in nanodiamond-polymer composites (nDPC) form ideal diffraction elements for very cold neutrons. Their advantage of high diffraction efficiency, combined with low angular selectivity as a two-port beam splitter, meets the necessary conditions for application in a very cold neutron interferometer. We provide an overview of the latest achievements in the construction of such a triple Laue interferometer. A first operational test of the interferometer is planned immediately after this conference in May 2025.

## I. INTRODUCTION

Half a century ago the first neutron interferometer with widely separated coherent beams based on Bragg diffraction from a perfect crystal boosted neutron optical and quantum mechanical experiments with (thermal) neutrons [1]. This kind of interferometer is akin to a Mach-Zehnder interferometer in light optics by replacing the beamsplitters as well as the mirrors with thick diffractive crystals in transmission geometry. While three equidistant and identical silicon crystal slabs, in the so called triple-Laue arrangement (LLL) with perfect alignment of the corresponding diffraction vectors, have been widely used for thermal neutrons (for an overview see Ref. [2, 3]), they cannot be used for neutrons with wavelengths exceeding twice the lattice spacing. To even enlarge the size, and thus the sensitivity, of the interferometer a split-crystal setup was successfully tested [4]. An extension beyond the thermal energies was established by using phase gratings [5–7] for very cold neutrons (VCN). Surface-relief gratings [8], multilayer mirrors [9] or artificial, holographically prepared thick gratings in photopolymers inspired by their thermal neutron counterpart were employed for the cold neutron regime [10, 11].

The sensitivity of an interferometer depends on the phase difference  $\Delta\Phi$  accumulated in either path [3]. For an LLL-type interferometer we aim at well separated paths which requires a long distance between each of the diffraction gratings. Here, we discuss our recent attempt to set up a new interferometer for the VCN regime with a total length of  $L = 1500$  mm, gratings with a spacing of  $\Lambda \approx 500$  nm and thus an estimated beam separation at the second grating of about 7.5 mm for VCN with a wavelength of 5 nm. Given a neutron beam with a certain characteristics there remain a vast number of severe challenges to assemble an LLL-interferometer for VCN (see Ref. [12]). Among them the most important ones are (1) the fabrication of appropriate gratings, and (2) their ultra-accurate alignment.

Our approach is to control the rotational alignment during the fabrication process of the gratings with respect to a precise reference granite plate, ensuring roll, pitch and yaw of each grating to be within about a  $\mu\text{rad}$ . This is sufficiently accurate according to detailed studies [13, 14] and also to our experience with an interferometer of similar type but shorter length ( $L = 300$  mm). [11, 15] A general overview on the requirements on artificial gratings for a VCN interferometer and the optimal choice of materials can be found in Ref. [16].

## II. PREPARATION OF GRATINGS AND LIGHT OPTICAL CHARACTERISTICS

Different groups of holographic materials were tested over the last 20 years for their applicability as efficient beamsplitters in cold neutron diffraction and VCN diffraction experiments [16–18]. Finally, nanodiamond polymer composites (nDPC) turned out to be the best choice for gratings used in a VCN interferometer [19–22]. To prepare the material we followed the formulation given in Ref. [23] except for replacing the photoinitiator with Rose Bengal

\* now at: Department of Physics and Astronomy, Uppsala University, Sweden

† send correspondence to M.F.: martin.fally@univie.ac.at

(RB), a dye that is photosensitive in the green optical region with a maximum of absorbance around 565 nm. A series consisting of more than hundred samples was prepared to optimize the grating quality with respect to recording light intensity, sample and grating thickness, pre- and post-exposure, and the concentration of the RB, respectively.

Fabrication of (volume) gratings for the VCN interferometer is performed as usual by holographic recording of two plane, s-polarized, coherent light waves which intersect at the nDPC sample position ( $2\theta \approx 61.2^\circ$ ). The used recording wavelength is  $\lambda_L = 514$  nm, the intensity at the position of the sample  $I = 200$  mW/cm<sup>2</sup>. This results in a one-dimensional periodic modulation, w.l.o.g. along the  $x$ -direction, of the refractive index for light. Light optical diffraction characteristics for the zero and first diffraction orders at Bragg matching condition during recording and after saturation and postcuring are shown in Fig. 1. The wavelength used for monitoring was  $\lambda_{L,\text{red}} = 632.8$  nm at which the nDPC syrup is insensitive.

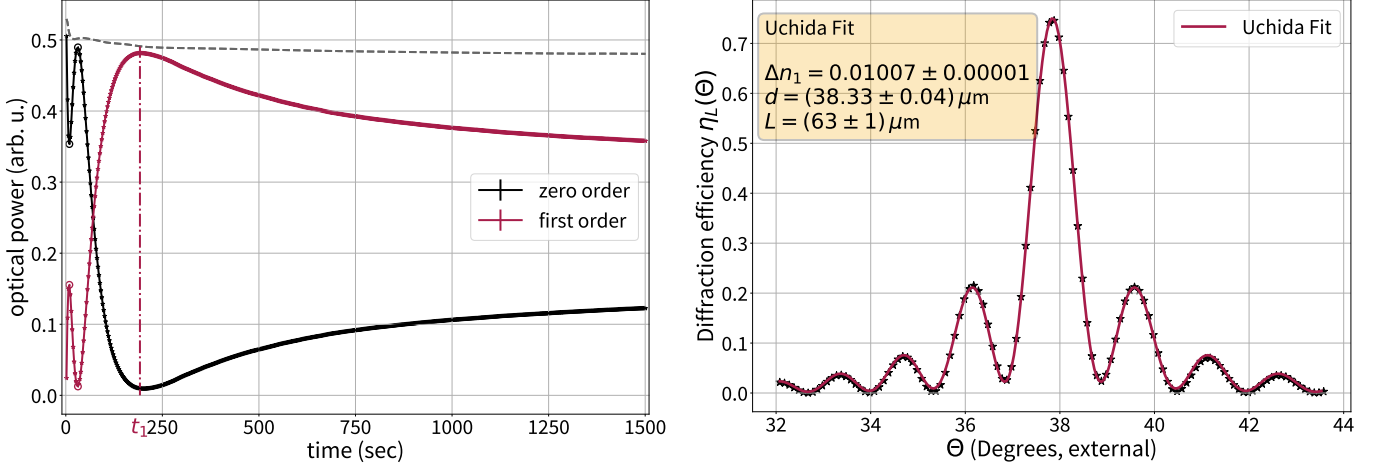


FIG. 1. *Left panel:* Buildup dynamics of the grating's first and zero order diffraction power (raw data) at Bragg matching condition as a function of recording time. The gray dashed line represents the total optical power. *Right panel:* Angular dependence of the diffraction efficiency  $\eta_L(\Theta)$  after saturation. The monitoring wavelength was  $\lambda_{L,\text{red}} = 632.8$  nm to which the holographic material nDPC is insensitive.

The temporal behaviour of grating formation has an initial phase with a rather fast increase in diffracted power, passing a maximum (at  $t \approx 10$  sec) followed by a minimum (at  $t \approx 30$  sec). This particular behavior of the grating buildup, as seen in Fig. 1, can be attributed to the emergence of a secondary grating which is due to the mutual diffusion of nanodiamonds and monomer, followed by the fast buildup and decay of a polymer grating (before monomer diffusion under holographic exposure) at high recording intensity (200 mW/cm<sup>2</sup>). The initial grating is in phase with the intensity-interference pattern, while the fundamental component of the secondary one experiences a  $\pi$ -phase shift because the refractive index of nanodiamonds is higher than that of the polymer formed.

Thereafter, the desired grating growth process ramps up and reaches the saturated value  $\Delta n_{\text{sat}} > 0.01$  at a photorefractive sensitivity  $S_{\eta 2} = 20$  cm/J, which is defined as the slope of  $\sqrt{\eta(t)}$  during the initial rise time, divided by intensity and thickness [24]. Note, that at  $t_1$  the grating becomes overmodulated for light. After recording and postcuring with a (white) LED lamp overnight, the angular dependence of the diffraction efficiency was measured. The result is shown in Fig. 1 together with a fit, accounting for a tentative exponential decay of the first order refractive-index modulation  $\Delta n_1(z)$  along the sample depth. It is notable, that in contrast to previously prepared nDPC gratings [22] apodization, i.e., the lifting of side minima, is negligible. This is expressed by an effective grating thickness  $L$  (i.e., the  $1/e$  value of the decaying grating along the thickness direction) which is much larger than the mechanical grating thickness  $d$ .

### III. NEUTRON OPTICAL CHARACTERISTICS

The recorded one-dimensional periodic structure of the formed gratings applies not only to light but also to neutrons for which it induces a modulation of the neutron-refractive index (or equivalently, the neutron optical potential). The latter can be written as  $n(x) = n_0 + 2|n_1| \cos(2\pi x/\Lambda + \varphi_1) + 2|n_2| \cos(4\pi x/\Lambda + \varphi_2) + \dots$ . For a majority of the materials under investigation the relative phases are  $\varphi_j \in \{0, \pi\}$ , thus  $\Delta n_j = \pm 2|n_j|$ ,  $\varphi \equiv 0$ . This is also the case for

nDPC, with  $\varphi_1 = \pi$  being the phase between the intensity pattern and the fundamental, first order Fourier component of the neutron-refractive index. The Fourier-coefficients  $n_j$  are related to the essential neutron optical parameter, the coherent scattering length density (SLD)  $b_c\rho$  by:

$$n_0 = \frac{\lambda^2[b_c\rho]}{2\pi}; \quad 2n_j = \Delta n_j = \frac{\lambda^2}{2\pi}\Delta[b_c\rho]_j, \quad j > 0. \quad (1)$$

Here we denote the Fourier coefficients of the light-induced changes of the SLD by  $\Delta[b_c\rho]_j$ .

The major advantage of an nDPC grating over other excellent light optical materials is their applicability for neutron diffraction. They have exceptionally large SLD modulation values  $\Delta[b_c\rho]_j$  which, together with the thickness  $d$  determine the maximum achievable diffraction efficiency at a given probe wavelength. Another important aspect is their negligible incoherent scattering.

For simplicity and as a rough estimation of diffraction efficiency<sup>1</sup> let us assume that diffraction takes place in the Bragg regime, in which only two waves with significant amplitudes are propagating [25]. Then the diffraction efficiency for Bragg-matched order  $m$  is approximately

$$\eta_m = \sin^2 \left( \frac{1}{2} d \lambda \Delta[b_c\rho]_m \right). \quad (2)$$

However, for realistic cases in VCN diffraction experiments, depending on  $d, \lambda$  and  $\Delta[b_c\rho]_j$ , diffraction takes place in a multiwave-coupling regime [26–28] and  $\eta_m$  is also determined by other Fourier coefficients  $\Delta[b_c\rho]_j$  with  $j \neq m$ . Together with the unavoidable wavelength distribution of the VCN beam this will lead to (usually) lower values than estimated by Eq. (2). Furthermore, in most practical cases, the magnitude of the Fourier coefficients decreases with increasing order  $j$ . Therefore, we intend to use only the first diffraction order with efficiency  $\eta_1$  in the interferometer. The second diffraction order with efficiency  $\eta_2$  might still be quite powerful as can be seen in Fig. 2. However, due to dephasing, i.e. deviation from perfect Bragg matching, the second order diffraction can be suppressed provided that  $\Lambda/d \approx \Theta_2 \approx \lambda/\Lambda$ . This is the case for choosing a thickness  $d \approx \Lambda^2/\lambda$ . For the VCN beamline with a (mean) wavelength of 5 nm and a grating period of 500 nm the optimal thickness thus is  $d = 50 \mu\text{m}$ . As can be seen from the angular dependence of the diffraction efficiencies  $\eta_m$  in Fig. 2, even a grating with a thickness of  $d \approx 40 \mu\text{m}$  is close enough to suppress higher orders. An accurate calculation requires the use of a theory considering more than two diffraction orders and the nonsinusoidal refractive index profile, e.g., a coupled wave analysis [26, 29].

The properties of the nDPC gratings were examined with VCN at the PF2/VCN beamline of the Institut Laue-Langevin ILL), Grenoble, France. We arranged a small angle diffraction experiment by collimating the VCN beam (mean wavelength:  $\lambda = 4.6$  nm) employing two rectangular slits with 1 mm width at a distance of 1220 mm resulting in a horizontal divergence of less than 2 mrad. The grating is placed on a rotation stage close to the end of the collimation. Finally, the 2D detector with  $2 \times 2 \text{ mm}^2$  pixel size is located 2280 mm downstream and allows to observe spots of all relevant diffraction orders ( $m = \pm 3, \pm 2, \pm 1, 0$ ). To prevent scattering of the VCN by air, the beam path is shielded with He-filled tubes. The diffraction efficiency of order  $m$  is defined as the neutron counts diffracted to order  $m$  divided by the sum of all counts:  $\eta_m = I_m / \sum I_m$ . To examine the properties of the grating we measured the counts of diffracted neutrons at a range of angular values  $\Theta$ ; data are made available by the ILL [30]. The subtraction of the background follows one or the other method presented in Ref. 28. The angular dependence of the resulting diffraction efficiencies is shown in Fig. 2 together with neutron count maps for two angular positions, either near the minus first or second order Bragg angle  $\Theta_{-1, -2}$ , respectively.

The nDPC grating shows excellent diffraction properties. For the first orders we find an efficiency of about 28% at the corresponding Bragg angles  $\Theta_1$  at which the second orders exhibit a minimum. This is important for the neutron flux economy when multiwave-coupling occurs. Note, that the measured diffraction efficiency is even higher than for gratings reported in a recent publication [22], as therein (1) the wavelength was longer, see Eq. 2, or/and (2) the grating was tilted by  $\zeta \approx 70^\circ$  about the its symmetry axis which leads to more than double effective thickness. While this latter approach is very useful, it is not applicable for an LLL-interferometer. We also prepared thicker gratings up to  $d \approx 60 \mu\text{m}$  with diffraction efficiencies of the untilted grating higher than 50%. However, when it comes to VCN one drawback at this thickness is the higher angular selectivity. Keeping in mind that the VCN beam has a rather broad wavelength distribution, part of the spectra will not be sufficiently diffracted. That is why slightly thinner gratings are chosen for the interferometer. After having fabricated three gratings, their mutual alignment is key to success. Perfectly aligned gratings with a flux maximized LLL interferometer and simultaneous highest contrast would be established for grating G1 and G3 a 50:50 beamsplitter, and G2 a mirror, respectively. By impressing a

---

<sup>1</sup> In neutron optics and interferometry usually the diffraction efficiency is termed *reflectivity*.

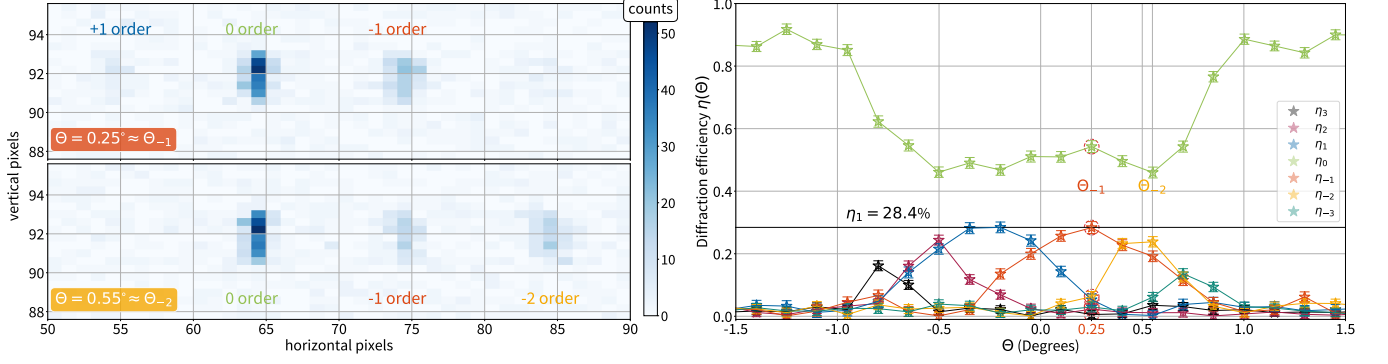


FIG. 2. *Left panel:* Part of the neutron count map on the detector matrix for two different angular positions (false colors, linear scale). The upper image shows the intensity map near the Bragg position  $\Theta_{-1}$  for the  $-1^{\text{st}}$  order, the lower one at  $\Theta_{-2}$  for the  $-2^{\text{nd}}$  order. *Right panel:* Angular dependence of the diffraction efficiency  $\eta(\Theta)$  for VCN. Diffraction orders between  $m = -3, \dots, +3$  with significant efficiency were detected. The circles mark  $\eta_m$  at the Bragg position  $\Theta_{-1}$  for which the neutron count map is shown in the upper left panel.

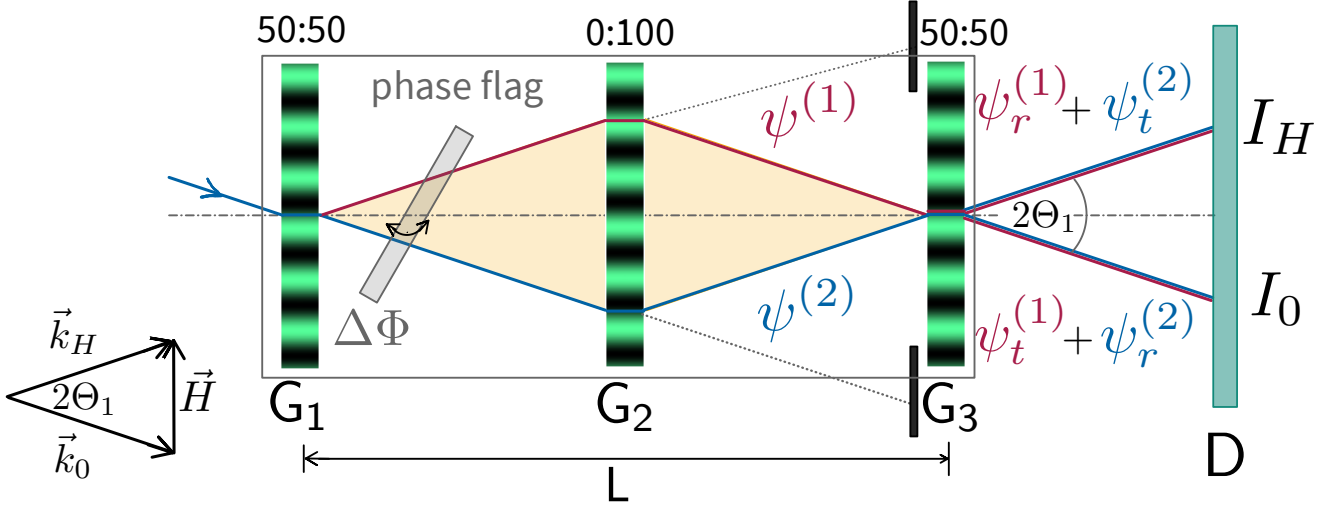


FIG. 3. Sketch of the VCN interferometer and beam paths therein. G1–G3 are the gratings, D denotes the detector and  $\psi^{(1)}, \psi^{(2)}$  are the wavefunctions for the corresponding path at G3. The subscripts  $r, t$  denote the wavefunctions reflected or transmitted from G3, respectively. The detected intensities are  $I_0 = |\psi_t^{(1)} + \psi_r^{(2)}|^2$  and  $I_H = |\psi_r^{(1)} + \psi_t^{(2)}|^2$ . Lower left drawing: the Laue condition, coining 0,  $H$  beam directions.

phase difference of  $\Delta\Phi$  between the two paths, maximum visibility  $v = (I_{\max} - I_{\min}) / (I_{\max} + I_{\min}) = 1$  for both pairs of the interfering beams with intensities  $I_H, I_0$ , respectively, are obtained (see sketch of beampaths in Fig. 3). For  $\eta_1 = \eta_3 = \eta$  but  $0 < \eta_2 < 1$  the visibility in the interfering beams travelling along 0-direction remains still perfect ( $v_0 = 1$ ), whereas the pair's visibility travelling along the  $H$ -direction is  $v_H(\eta) = 2\eta(1 - \eta) / [1 - 2\eta(1 - \eta)]$ . This is a realistic case. By shielding the beams forward-diffracted from G2, high visibility is possible, however, the experiment suffers from loss of neutron flux onto the detector.

#### IV. ALIGNMENT OF THE GRATINGS

Alignment of the three gratings is utmost delicate and requires ultra-accurate adjustment. Any deviation from perfect alignment and/or variation of the grating properties lead to a loss of contrast (visibility). Among them are:

deviation of the grating period for G1-G3, bent gratings, curved sample surface and their roughness; furthermore a deviation from equidistance between G1/G2 and G2/G3, pitch, yaw and roll angles. While all of them add up, the latter is the most critical one. To ensure less than 10% loss of contrast, the roll angle accuracy must not exceed a few microradians. Detailed discussions and estimated accuracy requirements can be found in [12–14, 31].

In a previously constructed interferometer for cold neutrons we mastered the alignment requirements by mounting the three samples of photosensitive deuterated poly(methyl)methacrylate equidistantly placed on a rigid breadboard, making it portable and deployable at different beamlines. To prepare the gratings each of the slabs was translated along the interferometer's symmetry axis into a standing light intensity pattern (two-wave mixing). After the translation and before exposing the next slab, the accuracy of the translation was detected by an autocollimation instrument (pitch, yaw) and a polarization optical setup sensitive to roll angle deviations [11, 15, 32]. This allowed us to successfully demonstrate the operation of the interferometer.

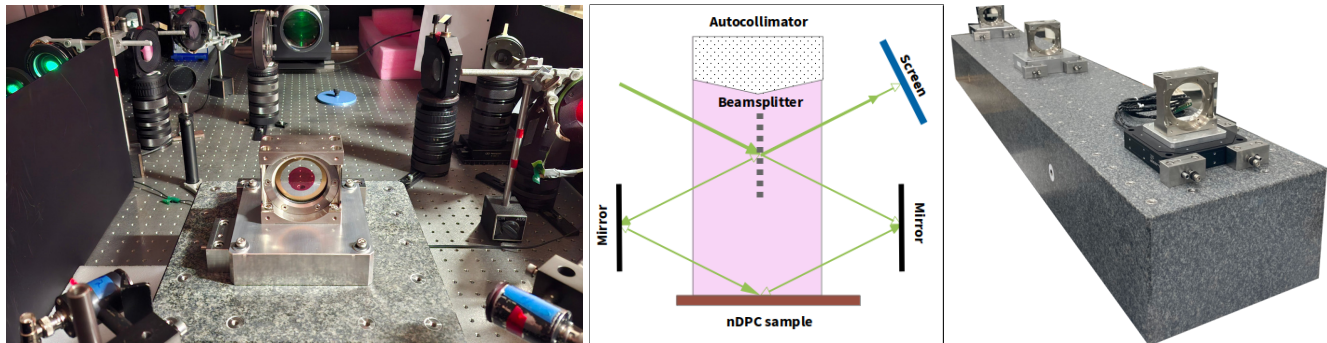


FIG. 4. *Left panel:* Picture of the optical recording. *Center panel:* Schematic of the adjustment setup, top view. Autocollimator and bisectrix of the recording angle are accurately in line within  $\mu\text{rad}$ . *Right panel:* The GB with roughly aligned sample holders. ©Fa. Johann Fischer, Aschaffenburg

To increase the size of the interferometer to  $L = 1.5\text{ m}$  we adopted a different approach. Removeable sample holders are placed on a super-planar plate of aluminum or a 6-axis nanopositioning stage for G3, respectively, which were adjusted on an extremely flat granite bench (GB) ( $300 \times 1760\text{ mm}^2$ ) by *Fa. Johann Fischer, Aschaffenburg*. The maximum deviation over the total area is less than half a micrometer; this defines the accuracy of roll and pitch angles. A shorter but otherwise identical twin of the granite bench ( $300 \times 300\text{ mm}^2$ ) is located on an optical table at the optical lab with a standard holographic two-wave mixing setup. The nDPC sample in its holder is placed on the granite and its surface-normal accurately aligned to form the bisectrix of the two holographic recording beams thereby defining zero yaw angle. Additionally we bring an autocollimation system (*Trioptics*) into line to exactly coincide with the bisectrix, which later serves as the reference when adjusting the gratings on the large bench at the neutron facility. A schematic and picture of the recording and adjustment setup are shown in Fig. 4. After recording of the gratings in nDPC they are transferred to PF2/VCN instrument and installed on the large GB, employing the autocollimation system for each of them to control and correct the yaw angle; pitch and roll angles are expected to fit. A picture of the GB and the sample holders in place during the calibration at *Fa. Johann Fischer* is shown in Fig. 4. The GB will be placed on a support, which can be moved on air cushions for positioning the VCN interferometer with respect to the neutron beam. A vacuum chamber will be designed to cover the interferometer and avoid scattering from air. The assembly and a first operational test are scheduled for May 2025.

## V. SUMMARY

We discussed the setup of an interferometer for VCN based on artificial gratings in the LLL-geometry. Gratings are holographically recorded in nDPC with desired grating period, thickness, and to a certain extent diffraction efficiency. The accurate mutual alignment of the gratings (within  $\mu\text{rad}$  in pitch, yaw and roll angles) in a VCN interferometer is accounted for by using a super-flat granite bench and an autocollimator. After successful setup results of a first operational test will be reported elsewhere.



## ACKNOWLEDGMENTS

Yasuo Tomita acknowledges a visiting professorship of the University of Vienna. Our special thanks go to Thomas Brenner who has provided us with crucial technical support on the very cold neutron beamline PF2/VCN over two decades. This research was funded in part by the Austrian Research Promotion Agency (FFG), Quantum-Austria NextPi, grant number FO999896034 and the European Union: "NextGenerationEU".

- 
- [1] H. Rauch, W. Treimer, and U. Bonse, "Test of a single crystal neutron interferometer," *Phys. Lett. A* **47**, p. 369, 1974. doi:10.1016/0375-9601(74)90132-7
  - [2] J. Klepp, S. Sponar, and Y. Hasegawa, "Fundamental phenomena of quantum mechanics explored with neutron interferometers," *Prog. Theor. Exp. Phys.* **2014**, August 2014. doi:10.1093/ptep/ptu085.
  - [3] H. Rauch and S. A. Werner, *Neutron interferometry*, Oxford University Press, New York–Oxford, 2nd ed., 2015. doi:10.1093/acprof:oso/9780198712510.001.0001.
  - [4] H. Lemmel, M. Jentschel, H. Abele, F. Lafont, B. Guerard, C. P. Sasso, G. Mana, and E. Massa, "Neutron interference from a split-crystal interferometer," *J. Appl. Crystallogr.* **55**, pp. 870–875, July 2022. doi:10.1107/s1600576722006082.
  - [5] M. Gruber, K. Eder, A. Zeilinger, R. Gähler, and W. Mampe, "A phase-grating interferometer for very cold neutrons," *Phys. Lett. A* **140**, p. 363, 1989. doi:10.1016/0375-9601(89)90068-6.
  - [6] K. Eder, M. Gruber, A. Zeilinger, R. Gähler, W. Mampe, and W. Drexel, "The new very-cold-neutron optics facility at ILL," *Nucl. Instrum. Meth. A* **284**, pp. 171–175, November 1989. doi:10.1016/0168-9002(89)90273-8.
  - [7] G. van der Zouw, M. Weber, J. Felber, R. Gähler, P. Geltenbort, and A. Zeilinger, "Aharonov-Bohm and gravity experiments with the very-cold-neutron interferometer," *Nucl. Instrum. Meth. A* **440**, pp. 568–74, 2000. doi:10.1016/S0168-9002(99)01038-4.
  - [8] A. Ioffe, V. Zabiyaikin, and G. Drabkin, "Test of a diffraction grating neutron interferometer," *Phys. Lett. A* **111**, pp. 373–375, September 1985. doi:10.1016/0375-9601(85)90373-1.
  - [9] H. Funahashi, T. Ebisawa, T. Haseyama, M. Hino, A. Masaike, Y. Otake, T. Tabaru, and S. Tasaki, "Interferometer for cold neutrons using multilayer mirrors," *Phys. Rev. A* **54**, p. 649, 1996. doi:10.1103/physrev.54.649.
  - [10] U. Schellhorn, R. A. Rupp, S. Breer, and R. P. May, "The first neutron interferometer built of holographic gratings," *Physica B* **234-236**, pp. 1068–1070, 1997. doi:10.1016/S0921-4526(97)00015-X.
  - [11] C. Pruner, M. Fally, R. A. Rupp, R. P. May, and J. Vollbrandt, "Interferometer for cold neutrons," *Nucl. Instrum. Meth. A* **560**, pp. 598–605, 5 2006. doi:10.1016/j.nima.2005.12.240.
  - [12] G. van der Zouw, *Gravitational and Aharonov-Bohm phases in Neutron Interferometry*. PhD thesis, Universität Wien, Austria, 2000.
  - [13] U. Schellhorn, *Anwendung holographischer Gitter in der Neutronenoptik*. PhD thesis, Universität Osnabrück, Germany, 1998. (in German).
  - [14] S. Breer, "Konstruktion und Aufbau eines LLL-Interferometers," Master's thesis, Universität Osnabrück, Germany, 1995. (in German).
  - [15] C. Pruner, *Ein Interferometer für kalte Neutronen*. PhD thesis, Universität Wien, Austria, 2004. (in German).
  - [16] M. Fally, J. Klepp, C. Pruner, E. Hadden, A. Bianco, J. Kohlbrecher, H. Filter, T. Jenke, and Y. Tomita, "Photosensitive materials for neutron optics," in *Photosensitive Materials and their Applications III*, R. R. McLeod, Y. Tomita, and I. Pascual Villalobos, eds., vol. 13015, p. 130150O, SPIE, June 2024. doi:10.1117/12.3022432.
  - [17] M. Fally, "The photo-neutronrefractive effect," *Appl. Phys. B* **75**, pp. 405–426, October 2002. doi:10.1007/s00340-002-1035-0.
  - [18] J. Klepp, C. Pruner, Y. Tomita, P. Geltenbort, J. Kohlbrecher, and M. Fally, "Holographic gratings for slow-neutron optics," *Materials* **5**, p. 2788, 2012. doi:10.3390/ma5122788.
  - [19] Y. Tomita, A. Kageyama, Y. Iso, K. Umemoto, M. Liu, J. Klepp, C. Pruner, T. Jenke, P. Geltenbort, and M. Fally, "Nanodiamond-polymer composite gratings as diffractive optical elements for light and neutrons I: their fabrication and light optical diffraction properties," in *Photosensitive Materials and their Applications*, R. R. McLeod, I. P. Villalobos, Y. Tomita, and J. T. Sheridan, eds., *SPIE Proc. Ser.* **11367**, p. 113670M, SPIE, 2020. doi:10.1117/12.2555651.
  - [20] M. Fally, J. Klepp, C. Pruner, T. Jenke, P. Geltenbort, A. Kageyama, Y. Iso, K. Umemoto, M. Liu, and Y. Tomita, "Nanodiamond-polymer composite gratings as diffractive optical elements for light and neutrons II: neutron optical diffraction properties," in *Photosensitive Materials and their Applications*, R. R. McLeod, I. P. Villalobos, Y. Tomita, and J. T. Sheridan, eds., *Proc. SPIE* **11367**, p. 113670N, SPIE, 2020. doi:10.1117/12.2555474.
  - [21] E. Hadden, Y. Iso, A. Kume, K. Umemoto, T. Jenke, M. Fally, J. Klepp, and Y. Tomita, "Nanodiamond-based nanoparticle-polymer composite gratings with extremely large neutron refractive index modulation," in *Photosensitive Materials and their Applications II*, R. R. McLeod, I. P. Villalobos, Y. Tomita, and J. T. Sheridan, eds., *Proc. SPIE* **12151**, pp. 1215109–1, SPIE, 2022. doi:10.1117/12.2623661.
  - [22] E. Hadden, M. Fally, Y. Iso, T. Jenke, J. Klepp, A. Kume, K. Umemoto, and Y. Tomita, "Holographic nanodiamond-polymer composite grating with unprecedented slow-neutron refractive index modulation amplitude," *Appl. Phys. Lett.* **124**(7), p. 071901, 2024. doi:10.1063/5.0186753.

- [23] Y. Tomita, A. Kageyama, Y. Iso, K. Umemoto, A. Kume, M. Liu, C. Pruner, T. Jenke, S. Roccia, P. Geltenbort, M. Fally, and J. Klepp, “Fabrication of nanodiamond-dispersed composite holographic gratings and their light and slow-neutron diffraction properties,” *Phys. Rev. Appl.* **14**, p. 044056, 2020. doi:10.1103/PhysRevApplied.14.044056.
- [24] H. Hatano, Y. Liu, and K. Kitamura, *Photorefractive Materials and Their Applications 2: Materials*, vol. 114 of *Springer Series in Optical Sciences*, ch. Growth and Photorefractive Properties of Stoichiometric LiNbO<sub>3</sub> and LiTaO<sub>3</sub>, pp. 127–164. Springer, New York, 2007. doi:10.1007/0-387-34081-5.
- [25] T. K. Gaylord and M. G. Moharam, “Thin and thick gratings: terminology clarification,” *Appl. Optics* **20**, pp. 3271–3273, 1981. doi:10.1364/AO.20.003271.
- [26] J. Klepp, C. Pruner, Y. Tomita, P. Geltenbort, J. Kohlbrecher, and M. Fally, “Advancing data analysis for reflectivity measurements of holographic nanocomposite gratings,” *J. Phys.: Conf. Ser.* **746**, pp. 012022:1–9, September 2016. doi:10.1088/1742-6596/746/1/012022.
- [27] M. Fally, Y. Tomita, A. Fimia, R. F. Madrigal, J. Guo, J. Kohlbrecher, and J. Klepp, “Experimental determination of nanocomposite grating structures by light- and neutron-diffraction in the multi-wave-coupling regime,” *Opt. Express* **29**, pp. 16153–16163, May 2021. doi:10.1364/oe.424233.
- [28] E. Hadden, *Polymer based photonic materials for cold neutron optics*. PhD thesis, Universität Wien, Austria, 2024. doi:10.25365/thesis.77766
- [29] M. G. Moharam, E. B. Grann, D. A. Pommet, and T. K. Gaylord, “Formulation for stable and efficient implementation of the rigorous coupled-wave analysis of binary gratings,” *J. Opt. Soc. Am. A* **12**(5), pp. 1068–1076, 1995. doi:10.1364/JOSAA.12.001068.
- [30] J. Klepp, M. Fally, H. Filter, T. Jenke, and C. Pruner, “Neutron diffraction from cyclic allylic sulfide based photopolymer film gratings.” doi:10.5291/ILL-DATA.3-14-445, 2024.
- [31] G. Drabkin, A. Ioffe, S. Kirsanov, V. Zabiyaikin, and M. Bedrizova, “Diffraction-grating interferometer for very cold neutrons: Questions of adjustment,” *Nucl. Instrum. Meth. A* **284**, pp. 176–178, November 1989. doi:10.1016/0168-9002(89)90274-x.
- [32] C. Pruner, R. Rupp, M. Fally, H. Dachraoui, R. Mazzucco, J. Zipfel, and R. P. May, “Interferometric measurement of the longitudinal coherence-function for cold neutrons,” in *ILL Annual Report 2002*, G. Cicognani and C. Vettier, eds., annual report Millennium Programm - New experimental techniques, p. 112, ILL, Grenoble, France, 2002.